P, *ρ*, *T* Measurements and Isobaric Vapor−Liquid−Equilibria of the 1,3,3-Trimethyl-2-oxabicycle[2,2,2]octane + Propan-1-ol Mixture: Cubic and Statistical Associating Fluid Theory-Based Equation of State Analysis

Marcos Torcal, Sandra García-Abarrio, Juan I. Pardo,* Ana M. Mainar, and José S. Urieta

Group of Applied Thermodynamics and Surfaces (GATHERS), Aragon Institute for Engineering Research (I3A), Facultad de Ciencias, Universidad de Zaragoza, Zaragoza 50009, Spain

Densities measured at pressures from (20 to 40) MPa and the temperatures (283.15, 298.15, 313.15, and 328.15) K and isobaric (vapor + liquid) equilibrium (VLE) at pressures of (33.33, 66.66, and 101.33) kPa are reported for the mixture {1,8-cineole(1,3,3-trimethyl-2-oxabicycle[2,2,2]octane) + propan-1-ol} in the whole composition range. Excess molar volumes, isobaric thermal expansions, and isothermal compressibilities were calculated from the density data. VLE data were correlated by means of three activity coefficient models [Wilson, nonrandom two-liquid (NRTL), and universal quasichemical activity coefficient (UNIQUAC)], and their thermodynamic consistency was determined. Four equations of state (EOS), namely, the Peng−Robinson, the Patel−Teja, statistical associating fluid theory (SAFT), and perturbed-chain statistical associating fluid theory (PC-SAFT), were used first to predict (interaction parameters, k_{ij}, equal to zero) both the density and the VLE behavior of the system and second to correlate the VLE by adjustment of the interaction parameters for each EOS.

Introduction

Supercritical fluid extraction of essential oils from plants with carbon dioxide as solvent is being extensively investigated. But in certain cases a polar cosolvent is added to the nonpolar carbon dioxide to improve the yields of the more polar compounds. The most usual cosolvents are alcohols such as ethanol or propan-1-ol.[1] It is then important to know the behavior of the mixtures (essential oil + cosolvent) to achieve better results in the supercritical extraction. Unfortunately, the essential oils are themselves complex mixtures. Nevertheless, the study of these systems can be carried out by choosing a major compound of the essential oil and mixing it with a cosolvent. This is the case of 1,8-cineole or eucalyptol (with the International Union of Pure and Applied Chemistry (IUPAC) systematic name of 1,3,3-trimethyl-2-oxabicycle[2,2,2]octane) that is the main component of the essential oil of hyssop (*Hyssopus officinalis* L.) amounting to 75 % of mass of the extract.[2] 1,8-Cineole is also a component of Spanish sage (*Salvia lavandulifolia* Vahl.).[3]

In a previous paper[4] we reported the values of density, speed of sound, refractive index, and excess molar enthalpy for the system (1,8-cineole + propan-1-ol) at (298.15 and 313.15 K) and atmospheric pressure. In this work we follow our study about this mixture. Then, the density of binary mixtures of 1,8-cineole with propan-1-ol were measured at four temperatures of (283.15, 298.15, 313.15, and 328.15) K and pressures from (20 to 40) MPa in steps of 5 MPa. The isobaric vapor + liquid equilibrium (VLE) of the mixture was determined at pressures of (33.33, 66.66, and 101.33) kPa. From the density measurements, the excess molar volumes, the isobaric thermal expansions, and the isothermal compressibilities were calculated. From the VLE, the activity coefficients and the excess molar Gibbs function were determined. These results were correlated using the Wilson, nonrandom two-liquid (NRTL), and universal quasichemical activity coefficient (UNIQUAC) equations.

An analysis of the results has also been carried out in terms of four equations of state (EOS), two of them cubic in the molar volume (Peng−Robinson and Patel−Teja) and the other two based on perturbation models (statistical associating fluid theory (SAFT) and perturbed-chain statistical associating fluid theory (PC-SAFT)). In the first place the EOS were used to predict the (p, ρ, T) and VLE behavior, considering that there was no effect due to the mixture (the interaction parameters for each model were set equal to zero). At the sight of the significant deviations occurring in the predictions, the interaction parameters were adjusted to provide a best fit of the experimental data with each EOS.

Experimental Section

Materials. 1,8-Cineole (mole fraction purity > 0.997), and propan-1-ol (mole fraction purity > 0.999) were supplied by Aldrich. Octane, which was used to calibrate the high pressure densimeter, was obtained from Fluka (mole fraction purity > 0.995). The stated purities of the chemicals were verified by measuring their normal boiling points and densities and comparing them with the literature values.[4−14] The experimental and bibliographic data are listed in Table 1 and show good agreement. All liquids were used without further purification.

Equipment. The device used to measure density is similar to other ones previously used by Sousa et al.[15] and Esteve et al.[16] and is based on a vibrating tube densimeter Anton Paar DMA 512-P for high pressures. A detailed description of the apparatus, together with the validation of the equipment, can be found in the literature.[17] The uncertainty in the temperature control is ± 0.01 K. The pressure of the system was controlled by a pressure transmitter (STW-A09) that can operate at pressures up to 70 MPa with an uncertainty of ± 0.1 % of full scale. The overall uncertainty in the reported density was

---

* Corresponding author. Telephone number: 34 976 762 386. Fax number: 34 976 761 202. E-mail: jupardo@unizar.es.

10.1021/je100577v

Table 1. Experimental and Literature Normal Boiling Points, T_b, and Densities, ρ, for the Pure Liquids at $T = 298.15$ K and $P = 0.1$ MPa

	ρ/kg·m^{-3}		T_b/K	
	exp.	lit.	exp.	lit.
1,8-cineole	920.68	920.24[a] 921.8[c] 920.29[e] 920.13[f]	449.2	449.2[b] 449.6[d]
propan-1-ol	799.94	800.64[a] 799.6[c] 799.75[g] 799.66[j] 799.91[k]	370.2	370.35[g] 370.93[h] 370.21[i]

[a] Ref 4. [b] Ref 9. [c] Ref 5. [d] Ref 10. [e] Ref 7. [f] Ref 8. [g] TRC. [h] Ref 13. [i] Ref 14. [j] Ref 11. [k] Ref 12.

estimated to be ± 0.5 kg·m^{-3}. The mole fractions of the mixtures of 1,8-cineole + propan-1-ol were determined gravimetrically with a Mettler Toledo AB265-S balance, whose precision is ± 10^{-5} g that leads to an uncertainty of ± 0.0001 in the mole fraction.

The VLE experiments were performed at constant pressure by means of an all-glass dynamic recirculating ebulliometer. It is a commercial unit (Pilodist model VLE 100) built in Germany by Fisher, and the procedure followed is very similar to that described by Dominguez et al.[18] The uncertainty in the pressure was of ± 0.05 kPa. The equilibrium (boiling) temperatures were measured using a Pt-100 probe with an uncertainty of ± 0.2 K. The compositions of both phases were determined by measuring the density of the samples at T/K = 298.15 and atmospheric pressure with a vibrating tube densimeter Anton-Paar DSA 5000 with which the densities of the mixture were previously measured for this purpose over the whole composition range. These values agree with those reported earlier by Alfaro et al.[4] The uncertainty of this densimeter is estimated to be ± 0.04 kg·m^{-3}. The relationship between the measured densities and the mole fraction is expressed through a Redlich−Kister type equation

$$\rho = x_1\rho_1 + x_2\rho_2 + \sum_{i=0}^{N} A_i(2x_1 - 1)^i \qquad (1)$$

where ρ is the density of the mixture, ρ_1 and ρ_2 are the densities of 1,8-cineole and propan-1-ol, respectively, and x_1 and x_2 are the mole fractions of the corresponding liquids. The A_i coefficients were estimated using the Levenberg−Marquardt's algorithm that was also used in all of the subsequent regression analyses in this work. These coefficients are reported in Table S1 of the Supporting Information as well as the standard deviation σ. The uncertainty in the mole fractions so determined is estimated to be ± 0.0005 for both phases.

Results and Discussion

Density Measurements and Derived Properties. Densities for both pure liquids 1,8-cineole and propan-1-ol and their binary mixtures were measured at four temperatures of (283.15, 298.15, 313.15, and 328.15) K and pressures from (20 to 40) MPa in steps of 5 MPa. The experimental results appear in Table 2. The absolute deviations between experimental and bibliographic data for propan-1-ol[19−21] are less than 0.16 % and for 1,8-cineole[5,17] are less than 0.25 %. For each composition, the densities of the compressed liquid were correlated with the modified Tait equation:[22]

Table 2. Density, ρ, as a Function of Temperature, Pressure, and Mole Fraction for 1,8-Cineole (1) + Propan-1-ol (2)

	ρ/kg·m^{-3}									
	P/MPa					P/MPa				
	20	25	30	35	40	20	25	30	35	40
x_1	T/K = 283.15					T/K = 298.15				
0	825.1	828.4	831.5	834.5	837.4	814.2	817.6	820.9	824.0	827.1
0.0499	839.5	842.9	845.8	848.9	851.6	828.6	831.8	835.1	838.1	841.2
0.1061	853.7	856.9	859.8	862.8	865.5	842.6	845.8	849.0	852.0	855.0
0.2029	873.3	876.4	879.3	882.3	885.0	862.0	865.2	868.4	871.4	874.4
0.3028	889.7	892.8	895.6	898.6	901.4	878.3	881.6	884.7	887.7	890.6
0.3955	901.8	905.0	907.9	910.7	913.5	890.5	893.7	896.7	899.8	902.7
0.4938	912.4	915.6	918.5	921.3	924.0	901.0	904.3	907.3	910.3	913.2
0.5904	921.2	924.4	927.3	930.1	932.9	909.7	912.9	915.9	918.9	921.9
0.7000	929.6	932.8	935.7	938.5	941.2	917.9	921.1	924.2	927.1	930.1
0.7915	935.7	938.9	941.7	944.6	947.3	923.9	927.1	930.2	933.2	936.1
0.8954	941.2	944.3	947.2	950.1	952.8	929.4	932.6	935.7	938.8	941.6
0.9332	942.9	946.1	949.0	951.8	954.5	931.1	934.3	937.3	940.3	943.3
1	945.9	949.1	952.0	954.9	957.6	934.1	937.4	940.5	943.4	946.4
x_1	T/K = 313.15					T/K = 328.15				
0	803.1	806.9	810.4	813.7	817.0	792.0	795.8	799.6	803.1	806.6
0.0499	817.1	820.8	824.3	827.5	830.7	805.9	809.7	813.3	816.8	820.2
0.1061	831.0	834.7	838.1	841.3	844.5	819.7	823.5	827.1	830.6	833.9
0.2029	850.4	854.0	857.4	860.7	863.9	838.9	842.6	846.3	849.6	853.1
0.3028	866.6	870.2	873.5	876.7	879.8	854.9	858.6	862.1	865.6	868.9
0.3955	878.6	882.2	885.5	888.7	891.7	866.9	870.5	874.0	877.4	880.9
0.4938	889.1	892.6	895.9	899.0	902.1	877.2	880.9	884.4	887.9	891.2
0.5904	897.7	901.2	904.5	907.6	910.8	885.9	889.6	893.1	896.5	899.9
0.7000	905.8	909.3	912.6	915.8	918.9	894.0	897.7	901.2	904.6	908.0
0.7915	911.8	915.3	918.6	921.8	924.9	899.9	903.7	907.2	910.5	913.9
0.8954	917.3	920.8	924.0	927.3	930.5	905.5	909.3	912.7	916.2	919.5
0.9332	919.1	922.5	925.9	929.1	932.2	907.3	911.0	914.5	917.9	921.3
1	922.3	925.8	929.1	932.4	935.5	910.6	914.3	917.9	921.3	924.7

Table 3. Coefficients of the Tait Equation for Pure Liquids and 1,8-Cineole (1) + Propan-1-ol (2) along with the Corresponding Standard Deviation of the Fitting[a]

	$x_1 = 0$	$x_1 = 0.0499$	$x_1 = 0.1061$	$x_1 = 0.2029$	$x_1 = 0.3028$
$a_0/\mathrm{kg \cdot m^{-3}}$	818.53	0.83332	0.84787	0.86798	0.88433
$a_1/\mathrm{kg \cdot m^{-3} \cdot K^{-1}}$	−0.7596	−0.7792	−0.7897	−0.7872	−0.7900
$a_2 \cdot 10^3/\mathrm{kg \cdot m^{-3} \cdot K^{-2}}$	−0.812	−0.757	−0.808	−0.808	−0.889
b_0/MPa	91.9	86.6	88.2	117.1	104.9
$b_1/\mathrm{MPa \cdot K^{-1}}$	−0.484	−0.458	−0.498	−0.625	−0.556
C	0.084	0.078	0.076	0.092	0.082
$\sigma/\mathrm{kg \cdot m^{-3}}$	0.08	0.11	0.09	0.07	0.11

	$x_1 = 0.3955$	$x_1 = 0.4938$	$x_1 = 0.5904$	$x_1 = 0.7000$
$a_0/\mathrm{kg \cdot m^{-3}}$	896.84	907.21	916.58	924.93
$a_1/\mathrm{kg \cdot m^{-3} \cdot K^{-1}}$	−0.7880	−0.7995	−0.8193	−0.8400
$a_2 \cdot 10^3/\mathrm{kg \cdot m^{-3} \cdot K^{-2}}$	−0.990	−1.020	−0.652	−0.500
b_0/MPa	117.0	91.8	121.4	105.1
$b_1/\mathrm{MPa \cdot K^{-1}}$	−0.609	−0.521	−0.631	−0.575
C	0.088	0.071	0.089	0.078
$\sigma/\mathrm{kg \cdot m^{-3}}$	0.10	0.08	0.11	0.07

	$x_1 = 0.7915$	$x_1 = 0.8954$	$x_1 = 0.9332$	$x_1 = 1$
$a_0/\mathrm{kg \cdot m^{-3}}$	930.81	936.57	938.49	940.68
$a_1/\mathrm{kg \cdot m^{-3} \cdot K^{-1}}$	−0.8400	−0.8384	−0.8471	−0.8420
$a_2 \cdot 10^3/\mathrm{kg \cdot m^{-3} \cdot K^{-2}}$	−0.525	−0.502	−0.315	−0.361
b_0/MPa	95.6	114.3	118.9	105.3
$b_1/\mathrm{MPa \cdot K^{-1}}$	−0.525	−0.605	−0.632	−0.571
C	0.072	0.083	0.085	0.079
$\sigma/\mathrm{kg \cdot m^{-3}}$	0.06	0.11	0.07	0.13

[a] $\sigma = [\sum_{i=1}^{N}(\rho_{i,\mathrm{exp}} - \rho_{i,\mathrm{calc}})^2/(N - P)]^{1/2}$; where N = number of experimental points and P = number of adjustable parameters.

$$\rho(P, T) = \rho(0.1\ \mathrm{MPa}, T)\left(1 - C(T)\ln\frac{B(T) + P/\mathrm{MPa}}{B(T) + 0.1\ \mathrm{MPa}}\right) \tag{2}$$

where $C(T)$ and $B(T)$ are temperature-dependent functions. In this work, $B(T)$ was given by:

$$B(T) = b_0 + b_1(T - T_0) \tag{3}$$

and C is assumed to be independent of temperature. $\rho(0.1\ \mathrm{MPa}, T)$ has the following dependence on the temperature:

$$\rho(0.1\ \mathrm{MPa}, T) = a_0 + a_1(T - T_0) + a_2(T - T_0)^2 \tag{4}$$

where $T_0/\mathrm{K} = 273.15$ and a_i have been considered as adjustable parameters. The densities $\rho(0.1\ \mathrm{MPa}, T)$ obtained from the adjustment deviate less than 3 % from experimental values at (298.15 and 313.15) K.[4] The coefficients of eqs 3 and 4 are listed in Table 3 along with the value of C and the standard deviation of the fitting for each composition. Figure 1a shows the measured densities and the smoothing equations for 1,8-cineole + propan-1-ol as a function of mole fraction of 1,8-cineole and pressure at the temperatures of (283.15 and 328.15) K.

Differentiating eq 2 with respect to temperature and pressure, the isobaric thermal expansion, α_P, and the isothermal compressibility, κ_T, can be determined. It is well-known[23] that analytical differentiation of the Tait equation with respect to pressure is certainly the most direct way to obtain reliable values of isothermal compressibility. The calculated isothermal compressibilities were estimated to have an expanded uncertainty

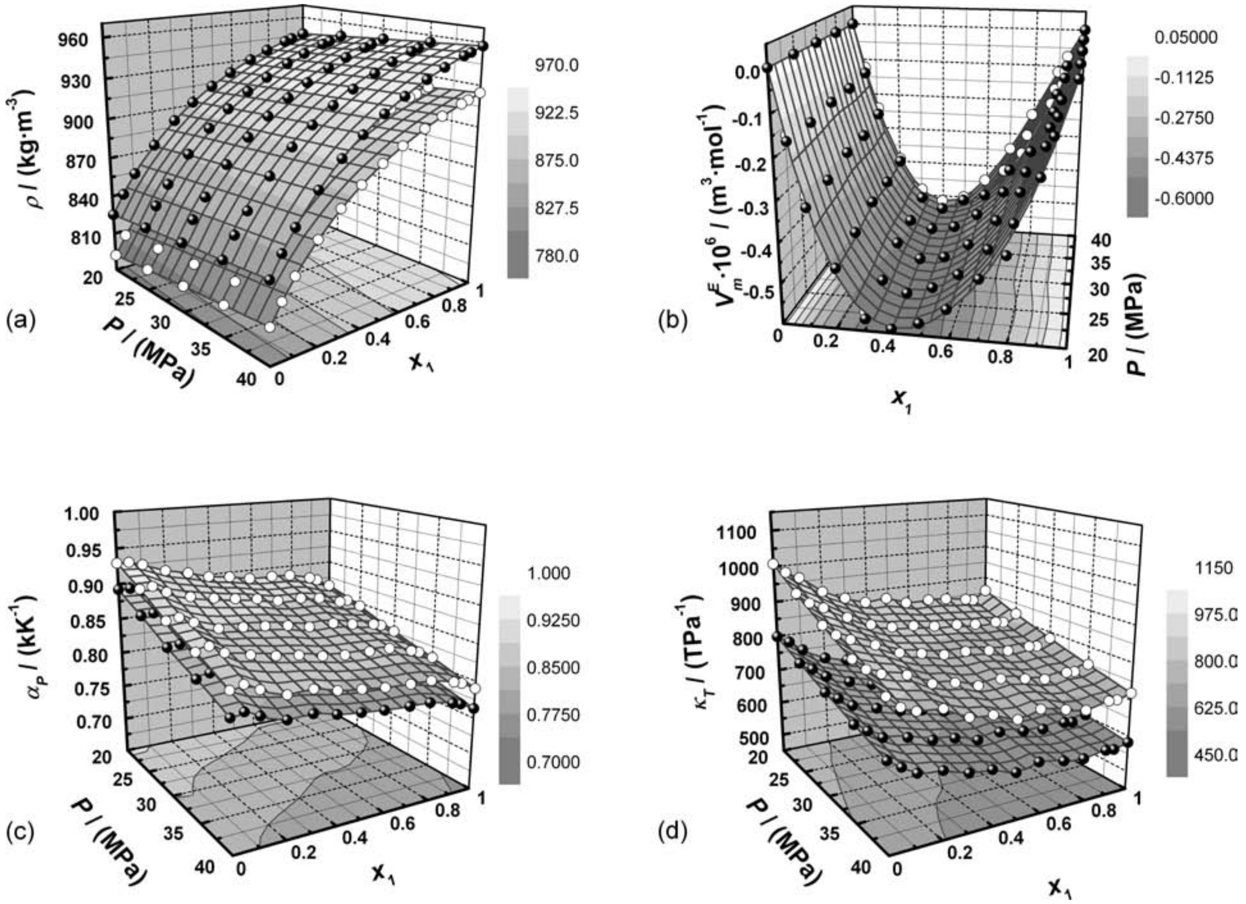

Figure 1. (a) Density, ρ, (b) excess molar volume, $V_{\mathrm{m}}^{\mathrm{E}}$, (c) isobaric thermal expansion, α_P, and (d) isothermal compressibility, κ_{T}, for 1,8-cineole (1) + propan-1-ol (2) as a function of mole fraction and pressure at the temperatures: ●, T = 283.15 K and ○, T = 328.15 K. Contour plots appear at the bottom of the figures.

Table 4. Parameters of the Redlich−Kister Polynomial, Equation 6, for the Excess Molar Volume, V_m^E, of 1,8-Cineole (1) + Propan-1-ol (2) along with the Corresponding Standard Deviations σ at the Given Pressure P and Temperature T[a]

	P/MPa				
	20	25	30	35	40
			T/K = 283.15		
$B_0 \cdot 10^6/\mathrm{m^3 \cdot mol^{-1}}$	−2.300	−2.263	−2.203	−2.129	−2.104
$B_1 \cdot 10^6/\mathrm{m^3 \cdot mol^{-1}}$	0.580	0.541	0.461	0.512	0.487
$B_2 \cdot 10^6/\mathrm{m^3 \cdot mol^{-1}}$	−0.68	−0.56	−0.44	−0.54	−0.41
$\sigma \cdot 10^6/\mathrm{m^3 \cdot mol^{-1}}$	0.01	0.01	0.01	0.01	0.01
			T/K = 298.15		
$B_0 \cdot 10^6/\mathrm{m^3 \cdot mol^{-1}}$	−2.417	−2.357	−2.259	−2.236	−2.175
$B_1 \cdot 10^6/\mathrm{m^3 \cdot mol^{-1}}$	0.650	0.655	0.625	0.532	0.564
$B_2 \cdot 10^6/\mathrm{m^3 \cdot mol^{-1}}$	−0.47	−0.25	−0.33	−0.42	−0.28
$\sigma \cdot 10^6/\mathrm{m^3 \cdot mol^{-1}}$	0.01	0.01	0.02	0.02	0.01
			T/K = 313.15		
$B_0 \cdot 10^6/\mathrm{m^3 \cdot mol^{-1}}$	−2.318	−2.267	−2.191	−2.098	−2.043
$B_1 \cdot 10^6/\mathrm{m^3 \cdot mol^{-1}}$	0.817	0.792	0.777	0.833	0.739
$B_2 \cdot 10^6/\mathrm{m^3 \cdot mol^{-1}}$	−0.14				
$\sigma \cdot 10^6/\mathrm{m^3 \cdot mol^{-1}}$	0.01	0.02	0.01	0.02	0.01
			T/K = 328.15		
$B_0 \cdot 10^6/\mathrm{m^3 \cdot mol^{-1}}$	−2.253	−2.166	−2.065	−2.033	−1.990
$B_1 \cdot 10^6/\mathrm{m^3 \cdot mol^{-1}}$	0.909	0.819	0.863	0.819	0.818
$B_2 \cdot 10^6/\mathrm{m^3 \cdot mol^{-1}}$		−0.24			0.14
$\sigma \cdot 10^6/\mathrm{m^3 \cdot mol^{-1}}$	0.01	0.02	0.02	0.01	0.01

[a]

$$\sigma = \sqrt{\sum_{i=1}^{N} (V_{\mathrm{m},i,\mathrm{exp}}^{\mathrm{E}} - V_{\mathrm{m},i,\mathrm{calc}}^{\mathrm{E}})^2/(N - P)}$$

where N = number of experimental points and P = number of adjustable parameters.

(calculated uncertainty multiplied by a coverage factor of 2) of ± 14 $\mathrm{TPa^{-1}}$. In a similar way, values of the isobaric thermal expansion could be determined from analytical calculation, but Cerdeiriña et al.[24] and Troncoso et al.[25] have found that the isobaric thermal expansion so estimated highly depends on the functions chosen for $B(T)$ and $\rho(0.1\ \mathrm{MPa}, T)$. Therefore, they recommend determining this property from the densities measured at constant pressure using a numerical procedure. Then, α_P was obtained in the pressure and temperature ranges following this procedure, and the expanded uncertainty of the values so determined is ± 0.005 $\mathrm{kK^{-1}}$. The calculated values of κ_T and α_P are given respectively in Tables S2 and S3 of Supporting Information. Figure 1c and d show κ_T and α_P for 1,8-cineole + propan-1-ol as a function of mole fraction of 1,8-cineole and pressure at the temperatures of (283.15 and 328.15) K.

Excess molar volumes were determined at each pressure and temperature using the relationship:

$$V_\mathrm{m}^\mathrm{E}(P, T) = x_1 M_1\left(\frac{1}{\rho} - \frac{1}{\rho_1}\right) + x_2 M_2\left(\frac{1}{\rho} - \frac{1}{\rho_2}\right) \qquad (5)$$

where M_1 and M_2 are the molar masses of 1,8-cineole and propan-1-ol, respectively. Table S4 of Supporting Information reports the calculated values of excess molar volumes. The estimated uncertainty of V_m^E is $\pm 5 \cdot 10^{-8}\ \mathrm{m^3 \cdot mol^{-1}}$. The V_m^E was fitted by means of the Redlich−Kister equation:

Table 5. Equilibrium Temperatures, T, Liquid Phase Mole Fractions, x_1, Vapor Phase Mole Fractions, y_1, Activity Coefficients, γ_i, and Reduced Excess Molar Gibbs Function, $G_\mathrm{m}{}^\mathrm{E}/RT$, of 1,8-Cineole (1) + Propan-1-ol (2)

T/K	x_1	y_1	γ_1	γ_2	$G_\mathrm{m}{}^\mathrm{E}/RT$	T/K	x_1	y_1	γ_1	γ_2	$G_\mathrm{m}{}^\mathrm{E}/RT$
					P/kPa = 33.33						
343.7	0.0084	0.0019	2.6093	0.9849	−0.0070	352.4	0.5250	0.0746	1.1038	1.3088	0.1797
343.8	0.0383	0.0079	2.3677	1.0049	0.0377	353.9	0.5806	0.0855	1.0714	1.3762	0.1739
344.8	0.1005	0.0178	1.9401	1.0174	0.0822	357.3	0.6412	0.1108	1.0864	1.3610	0.1637
345.2	0.1308	0.0217	1.7837	1.0303	0.1017	361.0	0.7394	0.1407	1.0246	1.5625	0.1342
345.6	0.1566	0.0254	1.7118	1.0394	0.1167	362.6	0.7671	0.1550	1.0186	1.6150	0.1258
346.9	0.2286	0.0355	1.5438	1.0624	0.1459	370.5	0.8493	0.2339	1.0138	1.6789	0.0897
348.4	0.3037	0.0468	1.4308	1.0900	0.1688	378.1	0.9045	0.3297	1.0071	1.7671	0.0607
349.1	0.3471	0.0518	1.3425	1.1220	0.1774	385.8	0.9404	0.4516	1.0065	1.7860	0.0407
350.1	0.4090	0.0588	1.2366	1.1790	0.1842	395.2	0.9731	0.6399	1.0023	1.9280	0.0199
351.3	0.4733	0.0670	1.1543	1.2463	0.1839	403.2	0.9912	0.8374	0.9972	2.0968	0.0038
					P/kPa = 66.66						
359.9	0.0239	0.0051	2.3804	0.9833	0.0043	375.0	0.6305	0.1079	1.0478	1.3289	0.1345
360.0	0.0621	0.0110	1.9668	1.0133	0.0544	378.0	0.6978	0.1306	1.0246	1.4265	0.1243
361.0	0.1178	0.0184	1.6634	1.0283	0.0845	382.9	0.7615	0.1696	1.0205	1.4626	0.1062
362.3	0.1894	0.0271	1.4439	1.0547	0.1128	386.9	0.8131	0.2072	1.0139	1.5630	0.0947
363.3	0.2470	0.0342	1.3411	1.0846	0.1337	392.7	0.8605	0.2663	1.0100	1.6132	0.0753
364.9	0.3234	0.0434	1.2181	1.1250	0.1435	400.0	0.9063	0.3562	1.0099	1.6908	0.0582
366.6	0.3943	0.0534	1.1482	1.1666	0.1478	405.8	0.9354	0.4393	1.0059	1.8077	0.0437
368.2	0.4649	0.0633	1.0834	1.2312	0.1486	409.6	0.9492	0.5017	1.0084	1.8383	0.0389
370.3	0.5192	0.0761	1.0742	1.2514	0.1450	417.4	0.9716	0.6454	1.0084	1.9009	0.0264
372.5	0.5761	0.0909	1.0623	1.2900	0.1427	428.8	0.9942	0.8949	0.9989	2.0783	0.0032
					P/kPa = 101.33						
370.3	0.0222	0.0036	1.7843	0.9858	−0.0012	382.7	0.5137	0.0787	1.0608	1.1944	0.1167
370.4	0.0421	0.0063	1.6397	0.9999	0.0207	385.2	0.5707	0.0947	1.0514	1.2250	0.1157
371.2	0.0872	0.0129	1.5711	1.0128	0.0510	387.8	0.6237	0.1118	1.0373	1.2612	0.1102
372.3	0.1369	0.0192	1.4276	1.0233	0.0686	393.1	0.7082	0.1501	1.0241	1.3187	0.0976
373.7	0.2032	0.0275	1.3057	1.0459	0.0900	397.6	0.7659	0.1878	1.0214	1.3713	0.0902
375.3	0.2715	0.0365	1.2209	1.0717	0.1046	405.1	0.8397	0.2592	1.0134	1.4705	0.0730
377.2	0.3478	0.0469	1.1408	1.1088	0.1132	413.2	0.8955	0.3537	1.0151	1.5770	0.0610
379.2	0.4165	0.0581	1.0962	1.1441	0.1168	419.1	0.9230	0.4325	1.0154	1.6121	0.0509
379.8	0.4357	0.0616	1.0870	1.1550	0.1176	427.8	0.9538	0.5677	1.0146	1.6515	0.0370
381.5	0.4836	0.0716	1.0702	1.1795	0.1181	440.5	0.9867	0.8090	1.0081	1.8964	0.0165

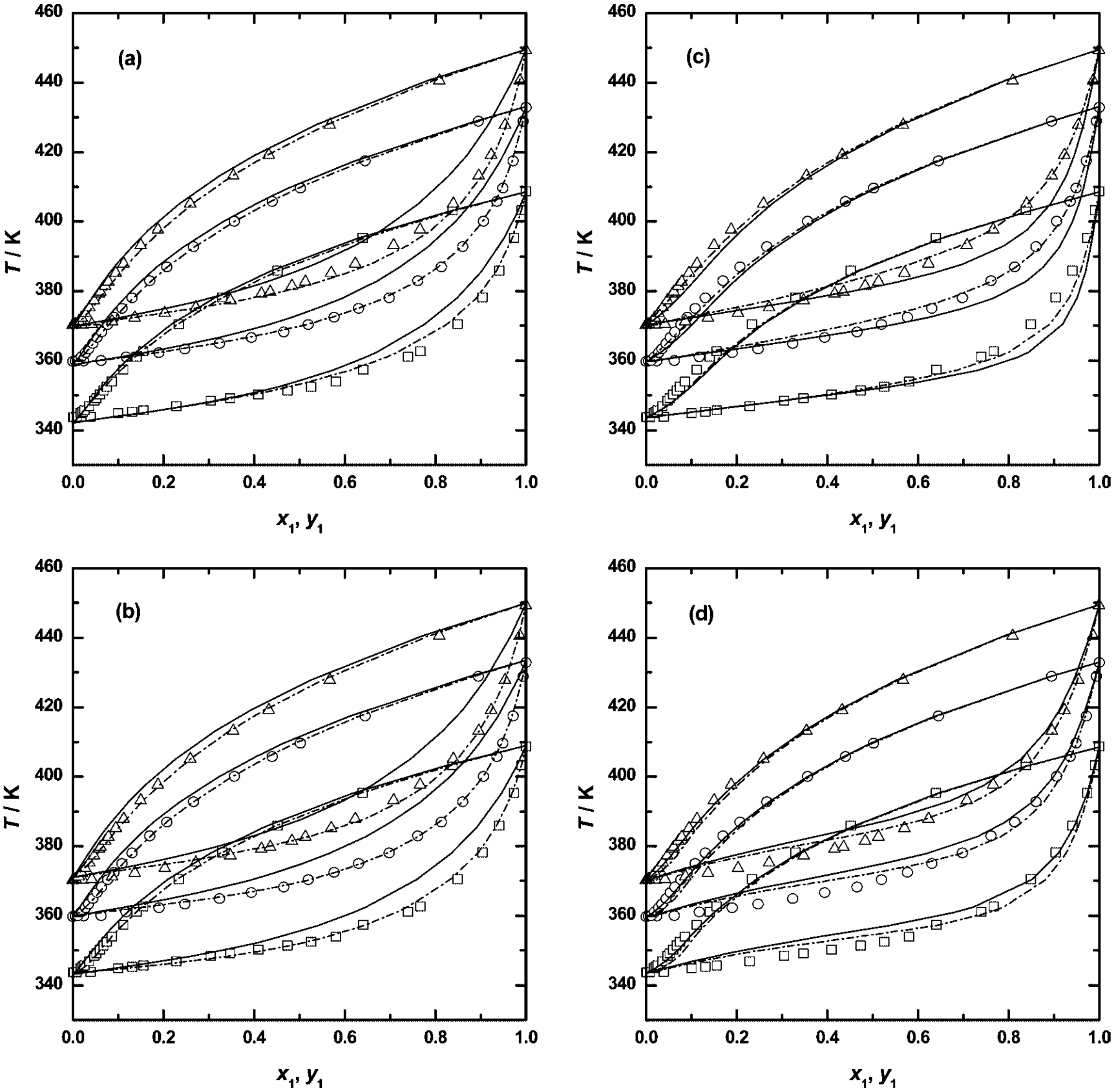

Figure 2. $T-x-y$ sections for the 1,8-cineole (1) + propan-1-ol (2): □, experimental data at $P = 33.33$ kPa; ○, experimental data at $P = 66.66$ kPa; △, experimental data at $P = 101.33$ kPa; —, predictions with $k_{ij} = 0$; — • — • —,correlations with k_{ij} adjusted to best represent the measured VLE. (a) Peng−Robinson; (b) Patel−Teja; (c) SAFT; (d) PC-SAFT.

$$V_m^E(P, T) = x_1x_2[B_0 + B_1(2x_1 - 1) + B_2(2x_1 - 1)^2] \tag{6}$$

where B_i are adjustable parameters whose values are listed in Table 4 along with the corresponding standard deviations of the fitting. The excess molar volumes and the correlation curves provided by eq 6 are shown at the temperatures of (283.15 and 328.15) K in Figure 1b as a function of the composition of 1,8-cineole and pressure. For all mixtures, V_m^E is negative over the whole temperature and pressure ranges as occurred at atmospheric pressure for the same system, indicating that the mixture is better packed than the pure compounds.[4] It is noticeable that V_m^E does not change with temperature in the pressure range studied.

Vapor−Liquid Equilibrium Determination. The isobaric VLE of the mixture 1,8-cineole + propan-1-ol was experimentally determined at the pressures of (33.33, 66.66, and 101.33) kPa. The experimental data, namely, equilibrium (boiling) temperatures and compositions of vapor and liquid phases, are gathered in Table 5 and plotted in Figure 2. From these data the activity coefficients (γ_i) were calculated according to the following equations:

$$\gamma_i = \frac{Py_i \exp\left[\frac{(V_i^0 - B_{ii})(P - P_i^{\text{sat}}) - (1 - y_i)^2 P\delta_{ij}}{RT}\right]}{P_i^{\text{sat}} x_i} \tag{7}$$

and

$$\delta_{ij} = 2B_{ij} - B_{ii} - B_{jj} \tag{8}$$

where x_i and y_i are the liquid and vapor mole fractions for the i component, P is the total pressure, T the temperature, P_i^{sat} the vapor pressure of component i at temperature T, V_i^0 the molar volume of component i, and R the universal gas constant. In eq 7 the B_{ii} and B_{ij} are the second virial coefficient of the pure liquids and the second cross virial coefficient, respectively: the virial coefficients were obtained from the correlation reported by Tsonopoulos.[26,27]

To obtain the vapor pressures of the components, the boiling temperatures of the pure components were also measured at several pressures, being the experimental data listed in Table

Table 6. Experimental Vapor Pressure of Pure Components

T/K	P^{sat}/kPa	T/K	P^{sat}/kPa
Propan-1-ol			
319.65	10.00	355.05	55.00
327.25	15.00	357.05	60.00
332.95	20.00	359.05	65.00
337.45	25.00	359.65	66.66
341.25	30.00	360.85	70.00
343.55	33.33	362.55	75.00
344.65	35.00	364.15	80.00
347.65	40.00	365.65	85.00
350.35	45.00	367.15	90.00
352.75	50.00	370.05	101.33
1,8-Cineole			
326.65	1.33	424.65	53.33
341.55	2.67	428.85	60.00
357.25	5.33	432.75	66.66
363.45	6.67	436.35	73.33
381.45	13.33	439.75	79.99
392.75	20.00	442.85	86.66
401.75	26.66	445.85	93.33
408.65	33.33	448.65	99.61
414.65	40.00	449.15	101.33
419.95	46.66		

Table 7. Coefficients for the Equations of Vapor Pressure. The Equation of Antoine Provides P^{sat}/kPa using T/K. Capital Letters: Equation of Antoine; Lower Case Letters: Wagner Equation

	A/a	B/b	C/c	d	T_{min}/K	T_{max}/K
1,8-cineole	13.9128	3523.60	−70.03		324.2	429.2
1-propanol[a]	−8.53706	1.96214	−7.6918	2.945		T_c

[a] Ref 14.

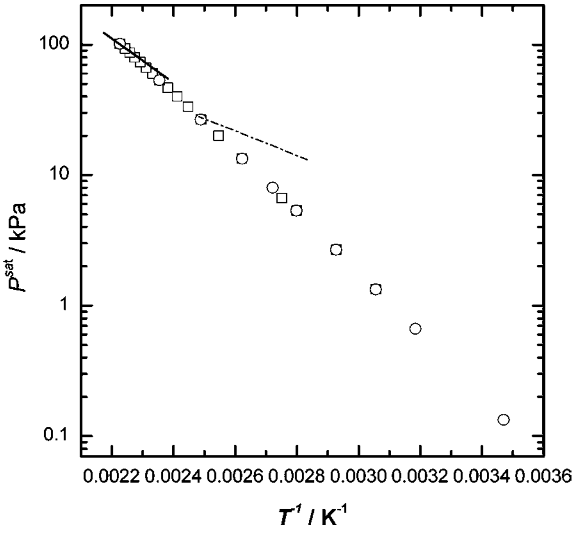

Figure 3. Vapor pressure P^{sat} of 1,8-cineole. □, experimental data; ○, by Stull;[9] —, by Farelo et al.;[10] − · −, by Hazra et al.[28]

6. For 1,8-cineole the vapor pressures were fitted to an Antoine equation that reproduces accurately the data. For calculations, the vapor pressure data of propan-1-ol were obtained from a Wagner equation taken from the literature.[12] This equation reproduces accurately our own measurements and allows us to obtain vapor pressures of propan-1-ol for temperatures above our experimental range. The values of the coefficients for both equations (Antoine and Wagner) are provided in Table 7. Figure 3 compares the measured vapor pressures for 1,8-cineole with values reported in the literature[9,10,28] as a function of the reciprocal of the temperature.

The excess molar Gibbs energy can be calculated from the activity coefficients using

$$\frac{G_{\text{m}}^{\text{E}}}{RT} = x_1 \ln(\gamma_1) + x_2 \ln(\gamma_2) \tag{9}$$

The values of the activity coefficients and the excess molar Gibbs energy are listed in Table 5. It can be seen that they are always positive, and then the system deviates positively from the Raoult law. This can be attributed to the prevailing effect of the breaking of the interactions existing in the pure compounds, breaking that is corroborated by the positive values of the excess enthalpy.[3]

Three activity coefficient models (Wilson,[29] NRTL,[30] and UNIQUAC[31]) were used to correlate the values reported in Table 6 by minimizing the objective function (OF)

$$\text{OF} = \sum_{j=1}^{m} \left[\left(\frac{\gamma_{1,j}^{\text{exp}} - \gamma_{1,j}^{\text{cal}}}{\gamma_{1,j}^{\text{exp}}} \right)^2 + \left(\frac{\gamma_{2,j}^{\text{exp}} - \gamma_{2,j}^{\text{cal}}}{\gamma_{2,j}^{\text{exp}}} \right)^2 \right] \tag{10}$$

where m is the total number of experimental data for each pressure, superscript exp refers to values obtained from eqs 7 and 8 and superscript cal refers to values calculated from one of the models (Wilson, NRTL, and UNIQUAC). The thermodynamic consistency of the experiments was determined by the van Ness method[32] described by Fredenslund et al.[33] that considers experimental data thermodynamically consistent if the average absolute deviation between calculated and measured vapor phase composition, Δy, is lower than 0.01. Table 8 shows the fitted parameters of the models (A_{ij}) and their average absolute deviation of the vapor phase composition (Δy) and temperature (ΔT). At the sight of these results, it can be concluded that the data are consistent.

Equations of State (EOS) Analysis. In this work two cubic EOS were used to describe the thermodynamic behavior of the mixtures: Peng−Robinson (PR)[34] and Patel−Teja (PT).[35] The properties of pure components needed to apply these equations are shown in Table 9. For 1,8-cineole critical properties were calculated according to Joback's method,[36] and the acentric factor estimated using the Lee−Kesler method,[37] whereas for propan-1-ol these properties were taken from literature.[13] The van der Waals mixing rule[13] was used to calculate the corresponding parameters for the mixture. The cross terms in the mixing rule were obtained from the classical quadratic combining rule.[13] The c parameter for the Patel−Teja EOS was taken as the arithmetical mean of c_1 and c_2 following the indications of Pfohl et al.[38] The equations corresponding to the mixing and combining rules can be found in the Supporting Information. To test the ability of the models to predict the high pressure liquid densities and the VLE, the interaction parameters k_{ij} and l_{ij} were considered equal to zero. The results obtained are listed in Tables S5 and S6 of the Supporting Information for high pressure liquid densities and in Tables S9 and S10 for the VLE.

The SAFT[39−41] and PC-SAFT[42,43] equations of state were also used to model the VLE and the $P-\rho-T$ behavior of 1,8-cineole + propan-1-ol. These equations account for the specific interactions between molecules, such as hydrogen bonds in carboxylic acid or alcohol groups. The parameters of the models for 1,8-cineole were evaluated from the correlation of our vapor pressure properties and liquid densities, while those for propan-1-ol were taken from literature.[39,43] All parameters are listed in Table 9.

In this work, van der Waals one-fluid mixing rules were used for SAFT and PC-SAFT. For the SAFT equation, the so-called

Table 8. Correlation Parameters for the Activity Coefficient Models, A_{ij} ($\lambda_{ij} - \lambda_{ii}$) for Wilson, Δg_{ij} for NRTL, and Δu_{ij} for UNIQUAC, Average Deviation in Vapor Phase Mole Fraction, Δy, and Average Deviation in Temperature, ΔT

model	A_{12}/J·mol^{-1}	A_{21}/J·mol^{-1}	Δy	ΔT/K
		P/kPa = 33.33		
Wilson	−312.76	3037.53	0.0041	0.3
NRTL[a]	332.80	2368.27	0.0035	0.3
UNIQUAC	1406.35	−726.65	0.0035	0.3
		P/kPa = 66.66		
Wilson	−932.39	3375.79	0.0065	0.6
NRTL[a]	311.63	2150.07	0.0066	0.6
UNIQUAC	1751.02	−1011.10	0.0053	0.5
		P/kPa = 101.33		
Wilson	−1950.67	3859.01	0.0062	0.7
NRTL[a]	860.77	960.51	0.0068	0.8
UNIQUAC	2124.84	−1343.72	0.0050	0.6

[a] $\alpha = 0.4$.

Table 10. Average Relative Deviations for Density (ARD %) and Average Absolute Deviations for Liquid and Vapor Phase (Δx and Δy) between Experimental Data and Those Calculated by EOS[a]

		Δx	Δy	Δx	Δy
EOS	ARD % ρ	$k_{ij} = 0$		$k_{ij} \neq 0$	
PR	3.02	0.0510	0.0119	0.0163	0.0039
PT	5.97	0.0775	0.0195	0.0149	0.0045
SAFT	4.93	0.0342	0.0142	0.0252	0.0086
PC-SAFT	0.95	0.0789	0.0061	0.0567	0.0126

[a]

$$\mathrm{ARD}\ \% = 1/N \sum_{i=1}^{N} |\rho_i^{\mathrm{exp}} - \rho_i^{\mathrm{cal}}|/\rho_i^{\mathrm{exp}}$$

$$\Delta z = 1/N \sum_{i=1}^{N} |z_i^{\mathrm{exp}} - z_i^{\mathrm{cal}}|$$

where N = total number of experimental points and z = liquid phase composition (x_1) or vapor phase composition (y_1).

vdW1 mixing rules[39] were applied to the segment energy, and for PC-SAFT the conventional Berthelot−Lorentz combining rules[42] were used. As in the case of the cubic EOS, the mixing and combining rules can be found in the Supporting Information. Tables S7 and S8 report the predictions (k_{ij} equal to zero) for the high-pressure liquid densities, and Tables S11 and S12 list the predicted VLE.

Figure 4 compares the density predicted from the four EOS with the experimental values at T/K = 283.15 and T/K = 328.15, while Figure 2 compares the VLE. Deviations between experimental data and predictions are reported in Table 10. The best density predictions are obtained from PC-SAFT with an average relative deviation (ARD) of 0.95 %. For the four EOS, the performance clearly depends on the accuracy of the prediction of the densities for the pure compounds. The PR equation underestimates the density of propan-1-ol (ARD = 2.81 %) but overestimates the density of 1,8-cineole (ARD = 6.00 %). For this reason, errors are compensated, and as a result the ARD = 3.02 % is obtained for the mixture. PT and SAFT overestimate the densities of both compounds. Because of this, higher deviations are found for PT and SAFT EOS (ARD = 5.97 % for PT and ARD = 4.93 % for SAFT). Referring to the

Table 9. Properties and Parameters of the Pure Components Used for the Application of the EOS

PR and PT		T_c/K		P_c/MPa		Ω
1,8-cineole		661.12[a]		3.019[a]		0.761[b]
propan-1-ol		536.98[c]		5.175[c]		0.629[c]
SAFT	m	v^{oo}/L·mol^{-1}	u^0/k/K	κ	ϵ/k/K	range T/K
1,8-cineole	5.4533	0.017607	247.83	0	0	327.25−449.15
propan-1-ol	3.240[d]	0.0120[d]	225.68[d]	0.01968[d]	2619[d]	293−493[d]
PC-SAFT	m_i	σ_i/Å	ϵ_i/k/K	$k^{A_iB_i}$	$\epsilon^{A_iB_i}$/k/K	range T/K
1,8-cineole	4.5346	3.8060	263.34	0	0	327.25−449.15
propan-1-ol	2.9997[e]	3.2522[e]	233.40[e]	0.015268[e]	2276.8[e]	240−537[e]

[a] Joback's method, ref 35. [b] Lee−Kesler method, ref 36. [c] Ref 13. [d] Ref 38. [e] Ref 42.

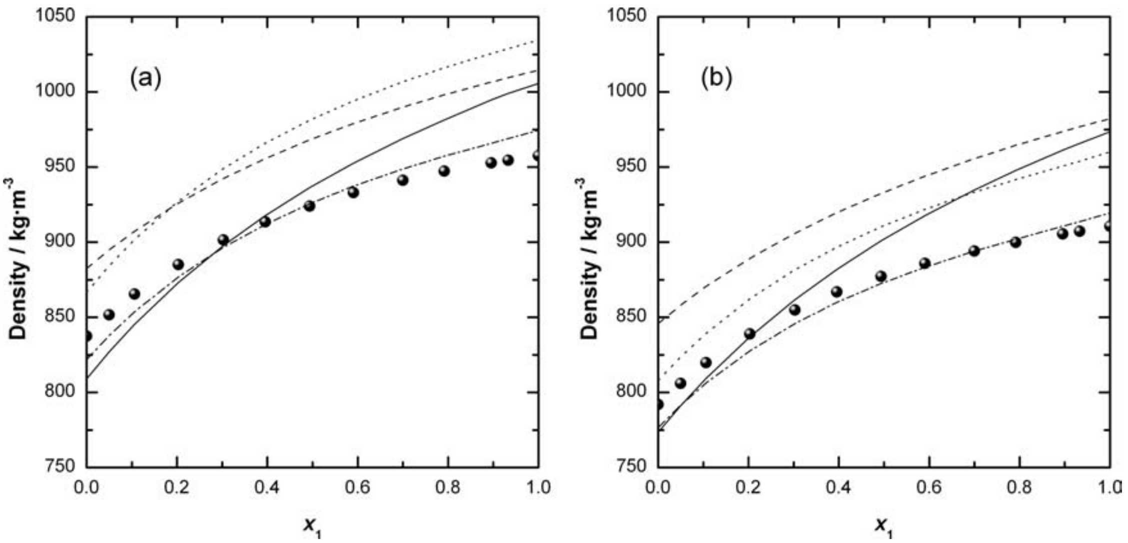

Figure 4. Density ρ of compressed mixture: ●, experimental data; —, Peng−Robinson; ····, Patel-Teja; ----, SAFT; — · — · —, PC-SAFT (a) at T = 283.15 K and P = 40 MPa and (b) at T = 328.15 K and P = 20 MPa.

Table 11. Binary Interaction Parameter for 1,8-Cineole (1) + Propan-1-ol (2) as a Function of Temperature T^a for Each EOS

EOS	k_{ij}
PR	$-4.12\cdot10^{-7}\cdot T^2 + 1.33\cdot10^{-3}\cdot T - 0.4113$
PT	$5.704\cdot10^{-6}\cdot T^2 - 3.53\cdot10^{-3}\cdot T + 0.5629$
SAFT	$5.442\cdot10^{-6}\cdot T^2 - 4.55\cdot10^{-3}\cdot T + 0.9260$
PC-SAFT	0.0106

[a] T in Kelvin.

VLE, the four EOS give good predictions for the dew points. However, significant deviations are found for bubble points. The best predictions are obtained by SAFT ($\Delta x = 0.0342$). Although the deviations for cubic EOS are lower than those for PC-SAFT ($\Delta x = 0.0789$), the shape of the $T-x-y$ diagrams obtained through PC-SAFT conforms more closely to the measured values. A reason for this is that in the propan-1-ol rich zone small errors in temperature lead to large errors in liquid phase composition.

Given the mentioned deviations between experimental values and those predicted by the EOS, the measured VLE were correlated with each EOS by adjusting the interaction parameters k_{ij} at each temperature and then fitting them to a simple polynomial function of temperature. In the case of the cubic EOS, the l_{ij} parameter was assumed equal to zero. The $k_{ij}(T)$ are listed in Table 11 for each EOS, and the results of these correlations are shown in Tables S13 to S16. The new dew and bubble lines can be found in Figure 2. The agreement between experimental and calculated values for the VLE is significantly improved by the use of the interaction parameters in the case of the cubic equations ($\Delta x = 0.0163$ for PR and $\Delta x = 0.0159$ for PT). The highest deviations ($\Delta x = 0.0567$) correspond, as before, to PC-SAFT that continues giving bubble points greater than the experimental values in propan-1-ol rich fluids.

Conclusions

Densities of 1,8-cineole + propan-1-ol were measured at the temperatures of (283.15, 298.15, 313.15, and 328.15) K and pressures from (20 to 40) MPa in steps of 5 MPa. The isobaric VLE of that mixture was also determined at pressures of (33.33, 66.66, and 101.33) kPa. Several derived properties were calculated from the experimental data. The excess molar Gibbs energy is positive over the whole composition range, pointing to the prevalence of a breaking of interactions. The excess molar volume is negative over the whole composition range indicating a better packing of the molecules in the mixture. The Peng−Robinson, Patel−Teja, SAFT, and PC-SAFT EOS have been used to predict both density and VLE. PC-SAFT leads to the better estimates of density, but in fact, none of the models performs satisfactorily for densities. The four EOS describe quite accurately the dew points but not the bubble points. For this reason, the interaction parameters were adjusted to better represent the experimental data resulting in a significant improvement in the estimated bubble points.

Supporting Information Available:

Mixing and combination rules used in EOS. Calculated values of the isothermal compresibilities, the isobaric thermal expansions, and the excess molar volumes for 1,8-cineole + propan-1-ol. $P-\rho-T$ predictions and VLE predictions and correlations of PR, PT, SAFT, and PC-SAFT equations of state. This material is available free of charge via the Internet at http://pubs.acs.org.

Literature Cited

(1) Taylor, L. T. *Supercritical Fluid Extraction*; John Wiley & Sons: New York, 1996.

(2) Langa, E.; Cacho, J.; Palavra, A. M. F.; Burillo, J.; Mainar, A. M.; Urieta, J. S. The evolution of hyssop oil composition in the supercritical extraction curve. Modelling of the oil extraction process. *J. Supercrit. Fluids* **2009**, *49*, 37–44.

(3) Langa, E.; Della Porta, D.; Palavra, A. M. F.; Urieta, J. S.; Mainar, A. M. Supercritical fluid extraction of Spanish sage essential oil: Optimization of the process parameters and modelling. *J. Supercrit. Fluids* **2009**, *49*, 174–181.

(4) Alfaro, P.; Langa, E.; Martínez-López, J. F.; Urieta, J. S.; Mainar, A. M. Thermophysical Properties of the Binary Mixtures (1,8-cineole + 1-alkanol) at T = (298.15 and 313.15) K and at Atmospheric Pressure. *J. Chem. Thermodyn.* **2010**, *42*, 291–303.

(5) Riddick, J. A.; Bunger, W. B.; Sakano, T. *Organic Solvents*, 4th ed.; John Wiley: New York, 1986.

(6) Aparicio, S.; Alcalde, R.; Dávila, M. J.; García, B.; Leal, J. M. Properties of 1,8-Cineole: A Thermophysical and Theoretical Study. *J. Phys. Chem. B* **2007**, *111*, 3167–3177.

(7) Barata, P. A.; Serrano, M. L. Densities and Viscosities of Thymol + 1,8-Cineole. *J. Chem. Eng. Data* **1994**, *39*, 298–301.

(8) Comelli, F.; Francesconi, M.; Castellari, C. Densities, Viscosities, and Excess Molar Enthalpies of Binary Mixtures Containing Essential Oils at (298.15 and 313.15) K. The (*S*)-(−)-Limonene + Cineole, (*S*)-(−)-Limonene + Linalool, and Cineole + Linalool Systems. *J. Chem. Eng. Data* **2001**, *46*, 868–872.

(9) Stull, D. R. Vapor Pressure of Pure Substances: Organic Compounds. *Ind. Eng. Chem.* **1947**, *39*, 517–540.

(10) Farelo, F.; Santos, F.; Serrano, L. Isobaric Vapor-Liquid-Equilibrium in Binary-Mixtures of α-Pinene, Limonene and 1,8-Cineole. *Can. J. Chem. Eng.* **1991**, *69*, 794–799.

(11) Langa, E.; Mainar, A. M.; Pardo, J.; Urieta, J. S. Excess Enthalpy, Excess Volume and Speed of Sound Deviation for the Mixture *β*-Pinene + Ethanol and *β*-Pinene + Propanol at (283.15, 298.15 and 313.15) K. *J. Chem. Eng. Data* **2005**, *50*, 1255–1261.

(12) Diaz Peña, M.; Tardajo, G. Isothermal Compressibilities of n-1-Alcohols from Methanol to 1-Dodecanol at 298.15, 308.15, 318.15, and 333.15 K. *J. Chem. Thermodyn.* **1979**, *11*, 441–445.

(13) Poling, B. E.; Prausnitz, J. M.; O'Connell, J. P. *The Properties of Gases and Liquids*, 5th ed.; McGraw-Hill: New York, 2007.

(14) Kato, M.; Kodama, D.; Abe, S.; Ohira, K.; Sato, M.; Sugiyama, K. Vapor-Liquid Equilibrium Behaviors of Coumarin and Vanillin in Ethanol, 1-Propanol, and 2-Propanol. *J. Chem. Eng. Data* **2006**, *51*, 1198–1200.

(15) Sousa, A. T.; de Castro, C. N.; Tufeu, R.; Le Neindre, B. Density of 1-Chloro-1,1-Difluoroethane (R142b). *High Temp. High Pressures* **1992**, *24*, 185–194.

(16) Esteve, X.; Conesa, A.; Coronas, A. Liquid Densities, Kinematic Viscosities, and Heat Capacities of some Alkylene Glycol Dialkyl Ethers. *J. Chem. Eng. Data* **2003**, *48*, 392–397.

(17) Lasarte, J. M.; Martín, L.; Langa, E.; Urieta, J. S.; Mainar, A. M. Set-up and validation of a *PρT* measuring device. Volumetric behavior of the mixture 1,8-cineole + ethanol. *J. Chem. Eng. Data* **2008**, *53*, 1393–1400.

(18) Dominguez, M.; Mainar, A. M.; Pardo, J.; Santafé, J.; Urieta, J. S. Experimental data, correlation and prediction of isobaric VLE for the ternary mixture (2-butanol + *n*-hexane + 1-chlorobutane) at 101.3 kPa. *Fluid Phase Equilib.* **2003**, *211*, 179–188.

(19) Watson, G.; Laffite, T.; Zéberg-Mikkelsen, C. K.; Baylaucq, A.; Bessieres, D.; Boned, C. Volumetric and Derivative Properties under Pressure for the System Propan-1-ol + Toluene: A Discussion of PC-SAFT and SAFT-VR. *Fluid Phase Equilib.* **2006**, *247*, 121–134.

(20) Abdulagatov, I. M.; Safarov, J. T.; Aliyev, F. Sh.; Talibov, M. A.; Shahverdiyev, A. N.; Hassel, E. P. Experimental Densities and Derived Thermodynamic Properties of Liquid Propan-1-ol at Temperatures from 298 to 423 K and at Pressures up to 40 MPa. *Fluid Phase Equilib.* **2008**, *268*, 21–33.

(21) Zuñiga-Moreno, A.; Galicia-Luna, L. A. Densities of Propan-1-ol and 2-Propanol via a Vibrating Tube Densimeter from 313 to 363 K and up to 25 MPa. *J. Chem. Eng. Data* **2002**, *47*, 155–160.

(22) Cibulka, I.; Hdnedkovsky, L. Liquid Densities at Elevated Pressures of n-Alkanes from C-5 to C-16: A Critical Evaluation of Experimental Data. *J. Chem. Eng. Data* **1996**, *41*, 657–668.

(23) Rowlinson, J. S.; Swinton, F. L. *Liquid and Liquid Mixtures*; Butterworths: London, 1982.

(24) Cerdeiriña, C. A.; Tovar, C. A.; González-Salgado, D.; Carballo, E.; Romaní, L. Isobaric Thermal Expansivity and Thermophysical Characterization of Liquids and Liquid Mixtures. *Phys. Chem. Chem. Phys.* **2001**, *3*, 5230–5236.

(25) Troncoso, J.; Bessières, D.; Cerdeiriña, C. A.; Carballo, E.; Romaní, L. Automated Measuring Device of (p, ρ, T) Data - Application to the 1-Hexanol plus *n*-Hexane System. *Fluid Phase Equilib.* **2003**, *208*, 141–154.

(26) Tsonopoulos, C. An Empirical Correlation of Second Virial Coefficient. *AIChE J.* **1974**, *20*, 263–272.

(27) Tsonopoulos, C.; Dymond, J. H. Second Virial Coefficient for Normal Alkanes, Linear 1-Alkanols (and Water), Alkyl Ethers, and Their Mixtures. *Fluid Phase Equilib.* **1997**, *133*, 11–34.

(28) Hazra, A.; Dollimore, D.; Alexander, K. Thermal analysis of the evaporation of compounds used in aromatherapy using thermogravimetry. *Thermochim. Acta* **2002**, *392*, 221–229.

(29) Wilson, J. M. Vapor-Liquid Equilibrium. XI. A New Expression for the Excess Free Energy of Mixing. *J. Am. Chem. Soc.* **1964**, *86*, 127–130.

(30) Renon, H.; Prausnitz, J. M. Estimation of Parameters for the NRTL Equation for Excess Gibbs Energies of Strongly Nonideal Liquid Mixtures. *Ind. Eng. Chem. Process Des. Dev.* **1968**, *8*, 413–419.

(31) Abrams, D. S.; Prausnitz, J. M. Statistical Thermodynamics of Liquid Mixtures - New Expression for Excess Gibbs Energy of Partly or Completely Miscible Systems. *AIChE J.* **1975**, *21*, 116–128.

(32) van Ness, H. C.; Byer, S. M.; Gibbs, R. E. Vapor−Liquid Equilibrium: Part I. An Appraisal of Data Reduction Methods. *AIChE J.* **1973**, *19*, 238–244.

(33) Fredenslund, A.; Gmehling, J.; Rasmussen, P. *Vapor−Liquid Equilibria Using UNIFAC*; Elsevier: Amsterdam, 1977.

(34) Peng, D. Y.; Robinson, D. B. A New Two Constant Equation of State. *Ind. Eng. Chem. Fundam.* **1976**, *15*, 59–64.

(35) Patel, N. C.; Teja, A. S. A New Cubic Equation of State for Fluids and Fluid Mixtures. *Chem. Eng. Sci.* **1982**, *37*, 463–473.

(36) Joback, K. G.; Reid, R. C. Estimation of Pure Component Properties of Pure Components from Group Contributions. *Chem. Eng. Commun.* **1987**, *57*, 233–243.

(37) Lee, B. I.; Kessler, M. G. Generalized Thermodynamic Correlation Based on 3-Parameter Corresponding States. *AIChE J.* **1975**, *21*, 510–527.

(38) Pfohl, O.; Petkov, S.; Brunner, G. “PE” Quickly Makes Available the Newest Equations of State Via the Internet. *Ind. Eng. Chem. Res.* **2000**, *39*, 4439–4440.

(39) Huang, S. H.; Radosz, M. Equation of State for Small, Large, Polydisperse and Associating Molecules. *Ind. Eng. Chem. Res.* **1990**, *29*, 2284–2294.

(40) Huang, S. H.; Radosz, M. Equation of State for Small, Large, Polydisperse and Associating Molecules: Extension to Fluid Mixtures. *Ind. Eng. Chem. Res.* **1991**, *30*, 1994–2005.

(41) Huang, S. H.; Radosz, M. Additions and Corrections to Equation of State for Small, Large, Polydisperse and Associating Molecules: Extension to Fluid Mixtures (vol 30, p 2002, 1992). *Ind. Eng. Chem. Res.* **1993**, *32*, 762.

(42) Gross, J.; Sadowski, G. Perturbed-Chain SAFT: An Equation of State Based on a Perturbation Theory for Chain Molecules. *Ind. Eng. Chem. Res.* **2001**, *40*, 1244–1260.

(43) Gross, J.; Sadowski, G. Application of the Perturbed-Chain SAFT Equation of State to Associating Systems. *Ind. Eng. Chem. Res.* **2002**, *41*, 5510–5515.

Received for review June 1, 2010. Accepted November 13, 2010. The authors thank the financial support of MICINN-FEDER (Project CTQ2009-14629-C02-02) and Gobierno de Aragón (PI068-08 and Group E-52). M.T. thanks GATHERS Group for his Fellowship for beginners.

JE100577V